

Evaluation of the Corrosion Inhibiting Effect of an Ionic Liquid (*N*-dimethyl-*N*-di(cocoalkyl) Ammonium Methyl Sulfate) on API 5L X52 Steel in Hydrochloric Acid

Paulina Arellanes-Lozada¹, Octavio Olivares-Xometl², Natalya V. Likhanova^{3,*}, Irina Lijanov⁴, M.A. Ramírez-Garnica², Elsa M. Arce-Estrada¹

¹Instituto Politécnico Nacional, ESIQIE, Departamento de Metalurgia y Materiales, Av. Instituto Politécnico Nacional S/N, Col. Lindavista, México D.F. 07300, México

²Facultad de Ingeniería Química, Benemérita Universidad Autónoma de Puebla, Av. San Claudio, Ciudad Universitaria. Col. San Manuel, Puebla, Pue. 72570, México

³Instituto Mexicano del Petróleo, Programa de Investigación y Posgrado, Eje Central Lázaro Cárdenas No. 152, Col. San Bartolo Atepehuacán, México D.F. 07730, México,

⁴Instituto Politécnico Nacional, CIITEC, Cerrada Cecati S/N, Colonia Santa Catarina, Azcapotzalco, México D.F. 02250, México

*E-mail: nvictoro@imp.mx,

Received: 26 November 2014 / Accepted: 15 January 2015 / Published: 19 January 2015

In the present work, the ionic liquid (IL) *N*-dimethyl-*N*-di(cocoalkyl) ammonium methyl sulfate (DCA) was tested as a corrosion inhibitor (CI). The tests were carried out in 1 M solutions of hydrochloric acid (HCl) in order to inhibit the corrosion of API 5L X-52 steel. The maximum inhibition efficiency (IE) was obtained at 4 h and 50 °C within the 96-99% interval and IE was obtained at 0 h and 30 °C within the 50-94% interval. The tests indicated that DCA inhibited the steel corrosion and worked as a mixed-type inhibitor, where the molecular adsorption on steel was described by the Langmuir isotherm, whereas thermodynamics suggested that a physisorption process occurred.

Keywords: Corrosion inhibitors; Acidic medium; Ionic liquids; Potentiodynamic polarization; Steel

1. INTRODUCTION

In most industrial processes, acidic solutions are commonly used for pickling, industrial acid cleaning, acid de-scaling, and they are also applied widely to enhance oil/gas recovery through acidification in the oil and gas industries [1]. Hydrochloric and sulfuric acids are the most common types of corrosive acids used in such industrial operations [2]. These types of acid solutions are very

aggressive and the main problem concerning API 5L X52 steel applications under different conditions in the industry is the loss of physical and chemical properties due to corrosion damage [3-5]. Several methods have been utilized in order to reduce the corrosion rate of API 5L X52 exposed to acidic solutions. The use of corrosion inhibitors (CIs) is a method used commonly to protect this steel type against corrosion damage [6]. By using CIs, it has been possible to preserve the integrity of metal components in facilities under severe corrosive conditions, which would normally lead to failure or a reduction in the operating cycle of essential equipment such as risers, columns and well structures, pipelines, distillation towers, and pressure vessels. For years, the organic compounds have proven to be excellent CIs in acid media and their high IEs are due mainly to their capacity of being adsorbed on the metallic surface. This adsorption phenomenon is favored by the presence of heteroatoms (nitrogen, sulfur, phosphorous and oxygen), functional groups and π bonds present in their molecular structure [6]. A problem regarding the application of inhibitors in different industries is that most of these compounds are toxic to humans and the environment. Currently, the search of new CIs is focused on "green corrosion inhibitors", where the ionic liquids (ILs) are found [7-10]. The ILs are organic salts that have a melting point below 100 °C. These compounds have a large number of advantageous physicochemical properties such as high ionic conductivity and non-flammability as well as chemical and thermal stabilities [11,12]. One of the most important characteristics of ILs is their negligible vapor pressure, which makes them eco-friendly and less hazardous inhibitors of metal corrosion [12,13]. The study of ILs as CIs is wide due to the ease that represents the combination of cations and anions for obtaining new CI molecules [13]. Derivatives of imidazolium [14-16], phosphonium [17], pyridinium [14,18,19], ammonium [20,21], and phosphonium [22] are some of the ILs that have been studied as CIs. This wide possibility of choosing cations and anions represents a good option for synthesizing new green CIs. The present work aims to investigate the corrosion inhibition effect of the IL *N*-dimethyl-*N*-di(cocoalkyl) ammonium methyl sulfate (DCA) on API 5L X52 steel in a 1 M HCl solution at different temperatures. The effect of the inhibitor concentration was evaluated by electrochemical tests, and scanning electron microscopy (SEM) was performed to evaluate the surface after exposure to the acid solution.

2. EXPERIMENTAL WORK

2.1 Preparation of Materials

The experiments were performed on API 5L X52 samples with a contact area of 0.28 cm². These materials were characterized and the following compositions (wt.%) were found: 0.08 C, 1.06 Mn, 0.26 Si, 0.019 P, 0.003 S, 0.0039 Al, 0.041 Nb, 0.018 Cs, 0.02 Cr, 0.019 Ni, 0.054 V, 0.003 Ti, 0.0002 Ca, 0.0003 B and the balance being Fe. The specimens were abraded with wet SiC paper number 400-600; afterwards, the specimens were degreased in hexane and washed in an ultrasonic bath of acetone for 5 min to remove impurities.

2.2 Test solutions

The test solutions were prepared by using standard grade hydrochloric acid and deionized water. This 1 M HCl aqueous solution was used to test the IL as CI of API 5L X52 steel.

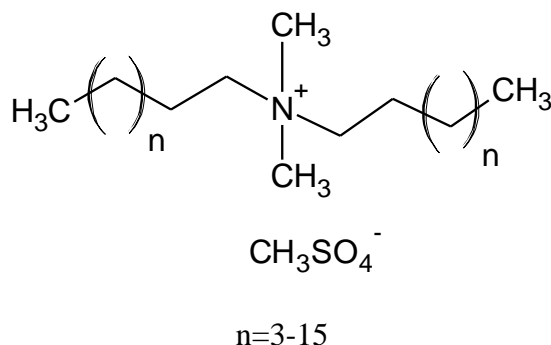


Figure 1. Structure of *N*-dimethyl-*N*-di(cocoalkyl) ammonium methyl sulfate (DCA) evaluated as CI.

Figure 1 shows the chemical name and abbreviation of the compound used in the present study, which was added to the acid solutions in concentrations of 10, 25, 50, 75 and 100 ppm (mgL^{-1}) to protect API 5L X52 steel from the corrosive media.

2.3 Electrochemical tests

Electrochemical measurements were carried out in a standard three-electrode cell. The electrode potential was measured against a saturated calomel electrode (SCE) via a Luggin capillary probe, which was used as the reference electrode. The counter electrode was a Pt mesh (99.9% purity) and the working electrode was made of API 5L X52 steel, which was embedded into a Teflon cylindrical bar. The tests were performed in a naturally aerated solution kept at temperatures of 25, 30, 40 and 50 °C. The electrochemical tests were carried out in a potentiostat/galvanostat PGSTAT302N controlled by a PC through the Nova 1.10 software. Before recording the electrochemical test polarization measurements, the working electrode was immersed in the test solution at steady-state open circuit potential (E_{OCP}) for 0, 4, 8 and 12 h right off the electrochemical test was done. The cathodic and anodic polarization curves were developed in the potential range from -250 mV to E_{OCP} , and from E_{OCP} to +250 mV at the same scanning rate of 0.166 mV s^{-1} . The reported data regarding the IE represent the average with a standard deviation of 0.3-3.5 %.

2.4 Surface analysis

The steel surface was recorded by a scanning electron microscope (SEM); images of the corroded surfaces and those after inhibitor addition were taken by a SEM Model JEOL-JSM-6300. Compositional results were obtained by using the EDX (Electron Dispersive X-ray) analysis module

attached to the microscope. The analyzed surfaces were exposed to OCP for 12 h at 25 °C and 4 h at 40 °C.

3. RESULTS AND DISCUSSION

3.1. Potentiodynamic Polarization

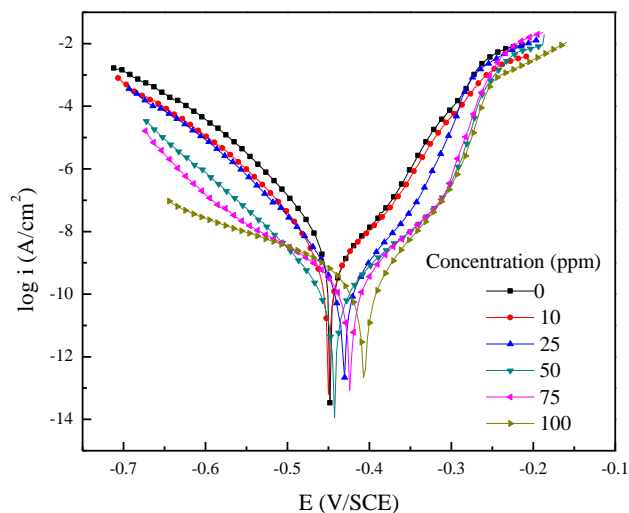


Figure 2. Tafel curves for API 5L X52 steel immersed in 1 M HCl in absence and presence of different DCA concentrations after 0 h of immersion at 30 °C.

The polarization curves of API 5L X52 steel in aqueous 1 M HCl, in the presence and absence of CI, are shown in Figures 2-4 at 30, 40 and 50 °C and different CI concentrations. The values of related electrochemical parameters i.e., corrosion potential (E_{corr}), corrosion current density (i_{corr}), cathodic Tafel slope (β_c) and inhibition efficiency (IE) were calculated and given in Tables 1 and 2. The IE was calculated from polarization measurements according to the relation given below:

$$IE (\%) = \left[1 - \frac{i_{corr}}{i_{corr}^0} \right] 100 \tag{1}$$

Where i_{corr} and i_{corr}^0 are inhibited and uninhibited corrosion current densities, respectively. The i_{corr} was obtained by the extrapolation of the current–potential lines to the corresponding corrosion potential.

In Figures 2-4, it can be clearly seen that the addition of inhibitor to the corrosive solution of 1 M HCl at the different temperatures reduces the anodic iron dissolution and also retards the cathodic hydrogen evolution reactions at the respective active sites; such a phenomenon is attributed to the increase in the covered surface degree (θ) prompted by the CI adsorption on the steel surface.

$$\theta = \left[\frac{100}{IE} \right] \tag{2}$$

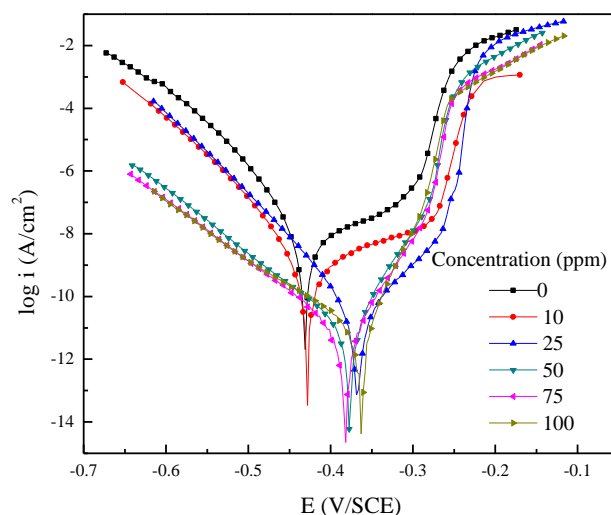


Figure 3. Tafel curves for API 5L X52 steel immersed in 1 M HCl in absence and presence of different DCA concentrations after 12 h of immersion at 40 °C.

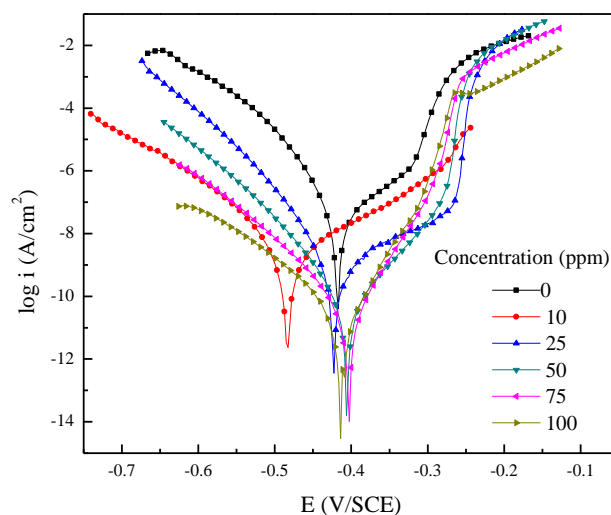


Figure 4. Tafel curves for API 5L X52 steel immersed in 1 M HCl in absence and presence of different DCA concentrations after 8 h of immersion at 50 °C.

The parallel cathodic Tafel lines (Figures 2-4) suggested that the addition of DCA inhibitor to the 1 M HCl solution do not modify the hydrogen evolution mechanism and the reduction of H^+ ions at the steel surface which occurs mainly through a charge transfer mechanism [23]. In Figure 2, the CI effect on the polarization curves at the different evaluated concentrations is observed clearly. These changes are more evident at concentrations above 25 ppm due to a higher presence of CI molecules, which provoke a decrease in the current density on the protected surface. Notwithstanding, as it can be observed in Figures 3 and 4, the anodic branches of the polarization curves obtained at 40 and 50 °C,

in presence and absence of CI, present clear adsorption and desorption processes regarding both corrosion products and CI molecules. Firstly, in CI absence, the formation of corrosion products such as Fe_3O_4 , $FeCl_2$ and hydrated oxides [24-27] is common. However, the solubility of this type of oxides localized on the steel surface is favored by the temperature effect. Therefore, it is logic to suppose that this corrosion product marks the pathway of the adsorption and desorption processes that are observed in the curves in the absence of CI, without forgetting that there is also a minor contribution by the other types of corrosion products occurring in such a process. Secondly, in CI presence, the adsorption and desorption processes are evident, but these processes become more complex due to the involved reactions between CI-oxides. On the one hand, on the steel surface, there are corrosion products of the same type as those obtained in CI absence, but in addition, there are also CI molecules whose role is more evident due to their adsorption on the active sites located on the zones where the corrosion products tend to be desorbed, a process that is confirmed by the decrease in the current intensity of the anodic and cathodic branches. Nevertheless, it has been reported that a temperature increase affects the CI adsorption on the metal surface to be protected [28]. In the present work, the potentiodynamic curves show clear displacements with respect to the current intensity in inhibitor presence with respect to the blank, being this displacement more evident at higher concentrations due to a higher concentration of molecules in the medium and on the surface, therefore, the corrosion velocity on the surface tends to be minor. This analysis is reflected specifically in the *IE* data reported in Table 1. Figure 5 shows the highest *IE* was obtained at 50 °C within the 96-99% interval for 4 h where the concentration did not influenced drastically the *IE*.

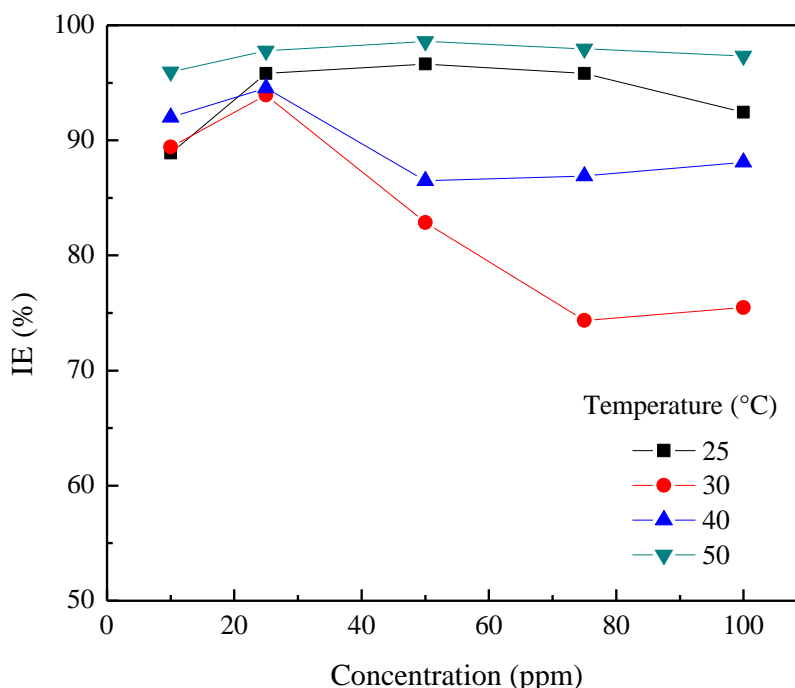


Figure 5. DCA inhibition efficiencies as CI of API 5L X52 steel in 1 M HCl after 4 h of immersion at different temperatures.

Table 1. Electrochemical parameters obtained from the Tafel curves of API 5L X52 steel immersed in 1 M HCl in absence and presence of different DCA concentrations at 25 and 30 °C.

Concentration (ppm)	Time (h)	25 °C				30 °C			
		β_c (mV/dec)	$-E_{corr}$ (mV/SCE)	I_{corr} ($\mu\text{A}/\text{cm}^2$)	IE (%)	β_c (mV/dec)	$-E_{corr}$ (mV/SCE)	I_{corr} ($\mu\text{A}/\text{cm}^2$)	IE (%)
0	0	146	471	688	-	137	449	897	-
	4	127	470	608	-	105	405	226	-
	8	124	479	313	-	106	411	317	-
	12	121	471	409	-	102	420	355	-
10	0	128	446	476	31	126	450	448	50
	4	109	479	67	89	84	409	24	89
	8	98	477	39	88	78	402	33	90
	12	48	472	76	81	76	411	58	84
25	0	121	468	338	51	124	431	255	72
	4	114	479	26	96	108	358	14	94
	8	101	477	24	92	78	390	22	93
	12	63	481	68	83	75	385	22	94
50	0	96	440	170	75	97	443	53	94
	4	142	379	20	97	199	368	39	83
	8	114	398	20	94	152	357	26	92
	12	107	415	21	95	99	373	13	96
75	0	97	427	131	81	143	423	59	94
	4	102	401	25	96	280	344	58	74
	8	103	412	24	92	293	343	62	81
	12	115	435	38	91	168	345	27	92
100	0	100	445	140	80	253	406	87	90
	4	119	432	46	92	326	390	55	76
	8	149	452	51	84	393	361	56	82
	12	171	420	34	92	347	349	40	89

By increasing the attack time of API 5L X52 steel in the solution, as observed in Figures 6 and 7, the *IE* changes become evident. In these figures, it is clear that DCA did not show high *IE* at very low concentrations. This fact may be attributed to the high solubility of the complexes formed between Fe^{n+} and DCA molecules. However, an increase in the DCA concentration caused a decrease in solubility of the complex, resulting in the formation of a more compact layer at the surface of the low carbon steel.

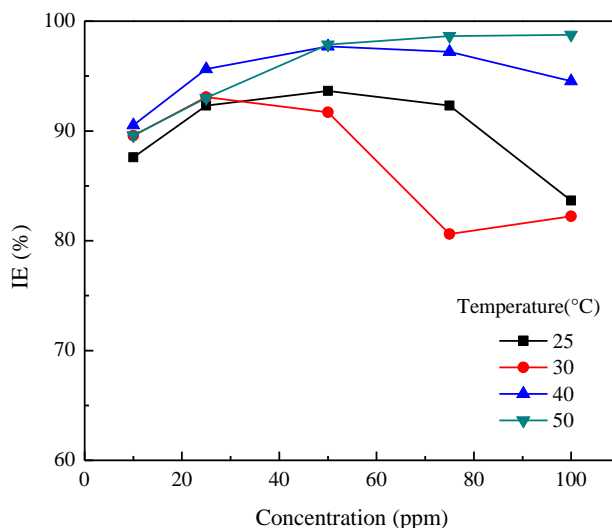


Figure 6. DCA inhibition efficiencies as CI of API 5L X52 steel in 1 M HCl after 8 h of immersion at different temperatures.

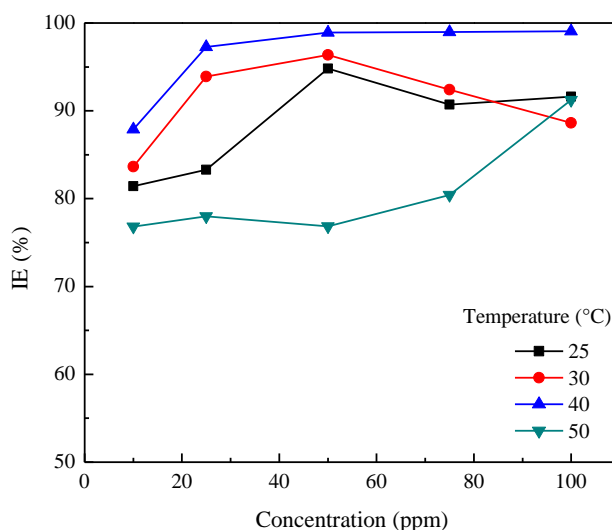


Figure 7. DCA inhibition efficiencies as CI of API 5L X52 steel in 1 M HCl after 12 h of immersion at different temperatures.

This process is linked directly to the adsorption of CI molecules on the surface as a time function, which is why that the maximum surface covered by the CI molecules is obtained after 4 h at the highest temperature due to the stability between the attraction and repulsion forces present in the surface-CI molecule interaction. This phenomenon, which is related to the *IE*, as observed in Table 2, leads to the formation of a protective film that is more homogeneous, stable and compact. Nevertheless, this film loses part of its properties eventually, as confirmed by Figure 7, due to energy

disequilibrium prompted by the oxidation-reduction reactions, which confirms that these ones can only be mitigated but controlled.

Table 2. Electrochemical parameters obtained from the Tafel curves of API 5L X52 steel immersed in 1 M HCl in absence and presence of different DCA concentrations at 40 and 50 °C.

Concentration (ppm)	Time (h)	40 °C				50 °C			
		β_c (mV/dec)	$-E_{corr}$ (mV/SCE)	I_{corr} ($\mu\text{A}/\text{cm}^2$)	IE (%)	β_c (mV/dec)	$-E_{corr}$ (mV/SCE)	I_{corr} ($\mu\text{A}/\text{cm}^2$)	IE (%)
0	0	132	426	988	-	154	413	2015	-
	4	116	397	426	-	155	403	3696	-
	8	115	421	835	-	147	418	3377	-
	12	125	431	1400	-	86	455	383	-
10	0	123	431	602	39	130	432	1389	31
	4	83	390	34	92	106	455	150	96
	8	84	403	79	91	156	484	352	90
	12	89	428	170	88	72	479	89	77
25	0	121	426	345	65	119	430	844	58
	4	93	365	23	95	91	396	82	98
	8	86	378	37	96	97	424	236	93
	12	88	369	38	97	70	467	84	78
50	0	86	437	93	91	101	428	434	78
	4	190	350	58	87	143	366	52	99
	8	118	365	19	98	104	406	72	98
	12	113	378	15	99	113	404	89	77
75	0	184	391	92	91	106	450	310	85
	4	308	335	56	87	221	356	76	98
	8	165	354	23	97	118	404	46	99
	12	118	382	14	99	123	420	75	80
100	0	246	379	139	86	200	447	294	85
	4	293	360	51	88	173	448	98	97
	8	269	341	46	95	146	415	42	99
	12	129	363	13	99	138	400	33	91

Some authors have reported that the kinetics of these redox reactions is accelerated by increasing the temperature, diminishing the IE as a result [28]. As for the present study, the IL-derived CI does not show such behavior, confirming once again the DCA properties with respect to those shown by ILs, which are stable within wide temperature intervals [7]. According to the aforesaid, the IE order as a time function is as follows: 0 h (31-94 %) < 4 h (74-99%) < 12 h (77-99%) < 8 h (81-99%). This order confirms that the maximum IE is obtained for any time interval at 8 h. Tables 1 and 2 show that the E_{corr} displacements do not feature a defined trend as a function of time and temperature. Initially, there is a preference toward the anodic zone, but with the increasing temperature, this

behavior is changed, which was observed at 0 and 8 h; the opposite case was observed at 4 and 12 h. According to Ahmed A. Farag [29], the classification of a compound as an anodic or cathodic inhibitor type is feasible when the OCP displacement is at least 85 mV in relation to the one measured for the blank solution. However, from Tables 1 and 2, the E_{corr} changes, positive and negative, are lower in inhibitor presence and lower with respect to the blank. These findings reveal that the investigated inhibitor decreased both the anodic iron dissolution and hydrogen evolution reaction by blocking the active sites, but they do not cause any appreciable changes in the E_{corr} values. Therefore, DCA evaluated as IL was classified as a mixed-type inhibitor.

3.2. Adsorption isotherms.

The corrosion inhibition process of steel in corrosive media by using ILs is explained frequently by means of the molecule adsorption process on the metallic surface, which prevent the adsorption of aggressive species present in the corrosive medium [15]. This statement is valid when the corrosion velocity is sufficiently small. Under this assumption, the adsorption equilibrium state tends to acquire a quasi-equilibrium state. This fact has allowed the use of different equilibrium adsorption isotherms in order to understand the inhibition process. In our case, different adsorption isotherm models such as Langmuir, Temkin, Freundlich, and Flory–Huggins were used, obtaining the best approximation with the Langmuir isotherm represented by equation (3):

$$\frac{C}{\theta} = \frac{1}{K_{ads}} + C \quad (3)$$

where C is the inhibitor concentration, K_{ads} is the equilibrium constant of the inhibitor adsorption process and θ is the surface coverage that was calculated by equation (2) from the data shown in Tables 1 and 2. Figure 8 shows the C/θ vs. C plot, where a good fitting process can be observed, which was obtained with correlation coefficient (R^2) data and the slope, which are reported in Table 3.

Table 3. Thermodynamic adsorption parameters of DCA on API 5L X52 steel in 1 M HCl.

Temperature (K)	R^2	Slope	K_{ads}	$-\Delta G_{ads}^{\circ}$ (kJ mol ⁻¹)
298.15	0.98	1.00	25,907	35.15
303.15	0.99	0.99	65,789	38.08
313.15	0.98	0.99	44,843	38.34
323.15	0.99	0.94	27,548	38.26

The slope values close to the unity confirm that the CI matches the criterion established by equation (3) and the formation of a CI monolayer on the steel surface is obtained. In addition, the high K_{ads} values indicate a fast adsorption process on the metal active sites. This phenomenon is due to the fast orientation of the high electronic density zone of the molecule located over the cation. In order to

confirm the interaction between the CI and the steel surface, the standard free adsorption energy, ΔG_{ads} , was calculated from equation (4):

$$\Delta G_{ads} = -2.303RT \log(55.5K_{ads}) \tag{4}$$

Where R is the gas constant, the 55.5 value is the molar concentration of water in the solution and T is the absolute temperature. The ΔG_{ads} values reported in Table 3 are found within the 35.15-38.34 kJ/mol interval at the used temperatures.

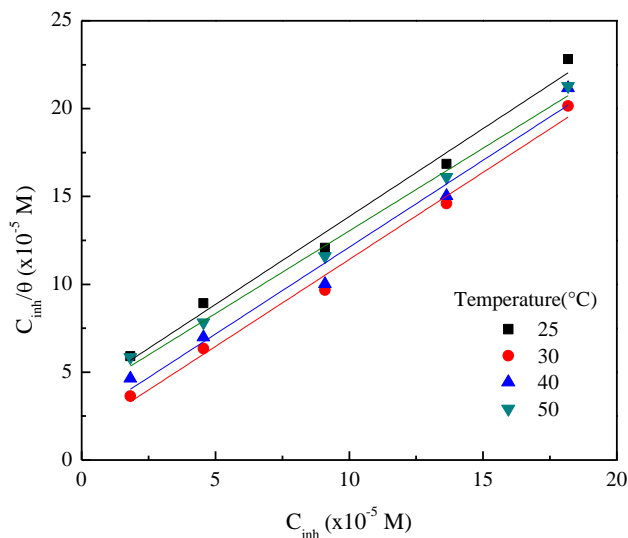


Figure 8. Langmuir isotherms for API 5L X52 steel in 1 M HCl at different temperatures for DCA.

This fact suggests that the metal surface exposed to the HCl solution is positively charged. The positively charged surface can attract Cl^- ions, which in turn will attract DCA molecules through electrostatic interactions. This causes the adsorption of a DCA complex on the metal surface, which prevents ferrous ions from entering the HCl solution.

3.3 SEM Analysis

SEM micrographs and the corresponding EDX spectra (Figure 9 and 10) of API 5L X52 steel surfaces were obtained to analyze the morphological change happening during the corrosion process in absence and presence of inhibitor as shown in these Figures.

Figure 9 (a) shows the steel surface before being submitted to the acid medium. This surface features a uniform morphology characteristic of a metallographic preparation. Its EDX spectrum shows the characteristic iron peaks. The steel morphology after 12 h of immersion at 25 °C in 1 M HCl without CI is shown in Figure 9 (b), where a dense layer of corrosion products with irregular morphology and evident cracks through which the aggressive ions present in the corrosive medium are diffused toward the steel surface, accelerating the mass loss.

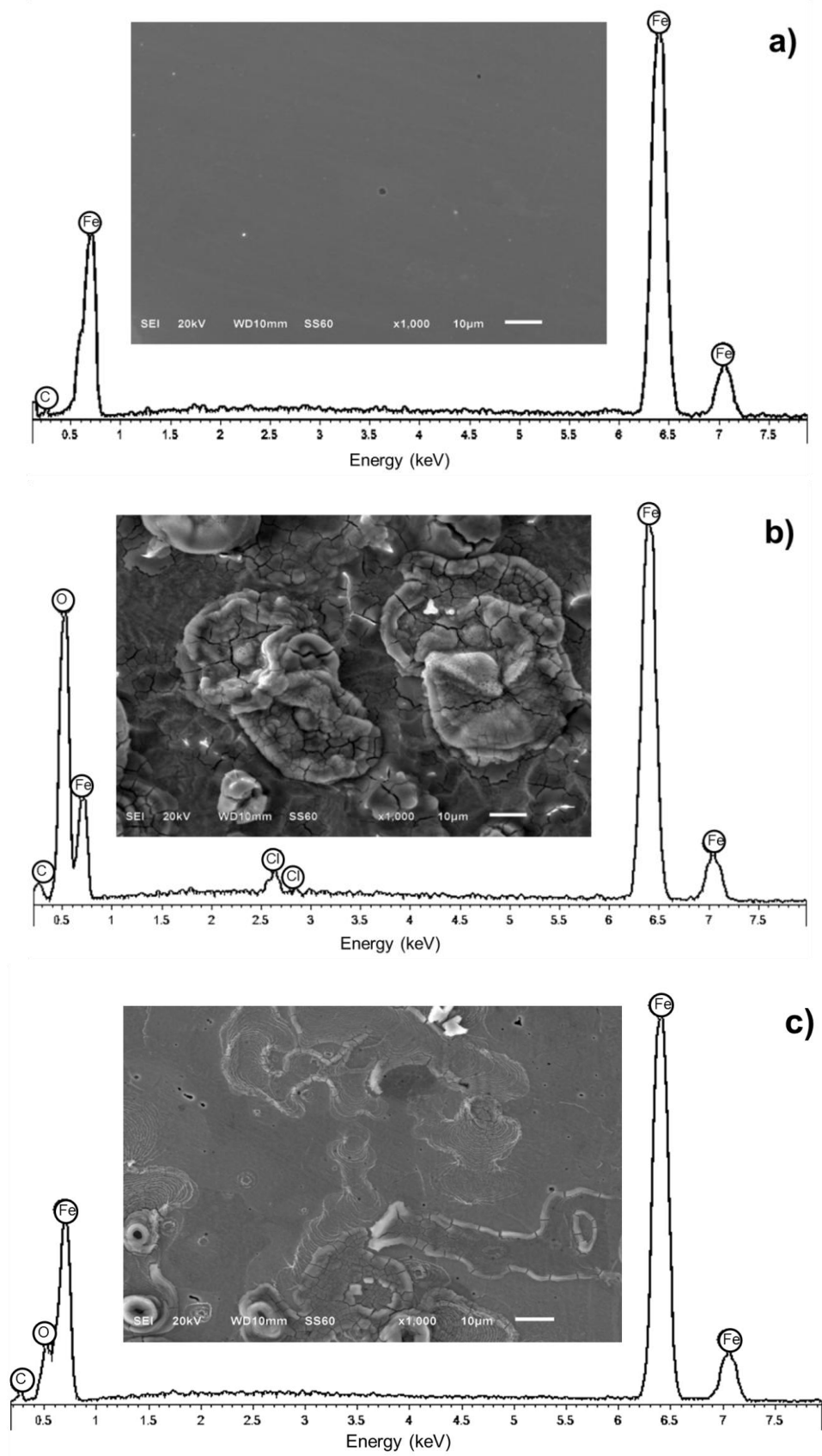


Figure 9. SEM micrographs and EDX spectrum for API 5L X52 steel after polishing (a), after 12 h of immersion in 1 M HCl in absence (b) and presence of 75 ppm of DCA (c).

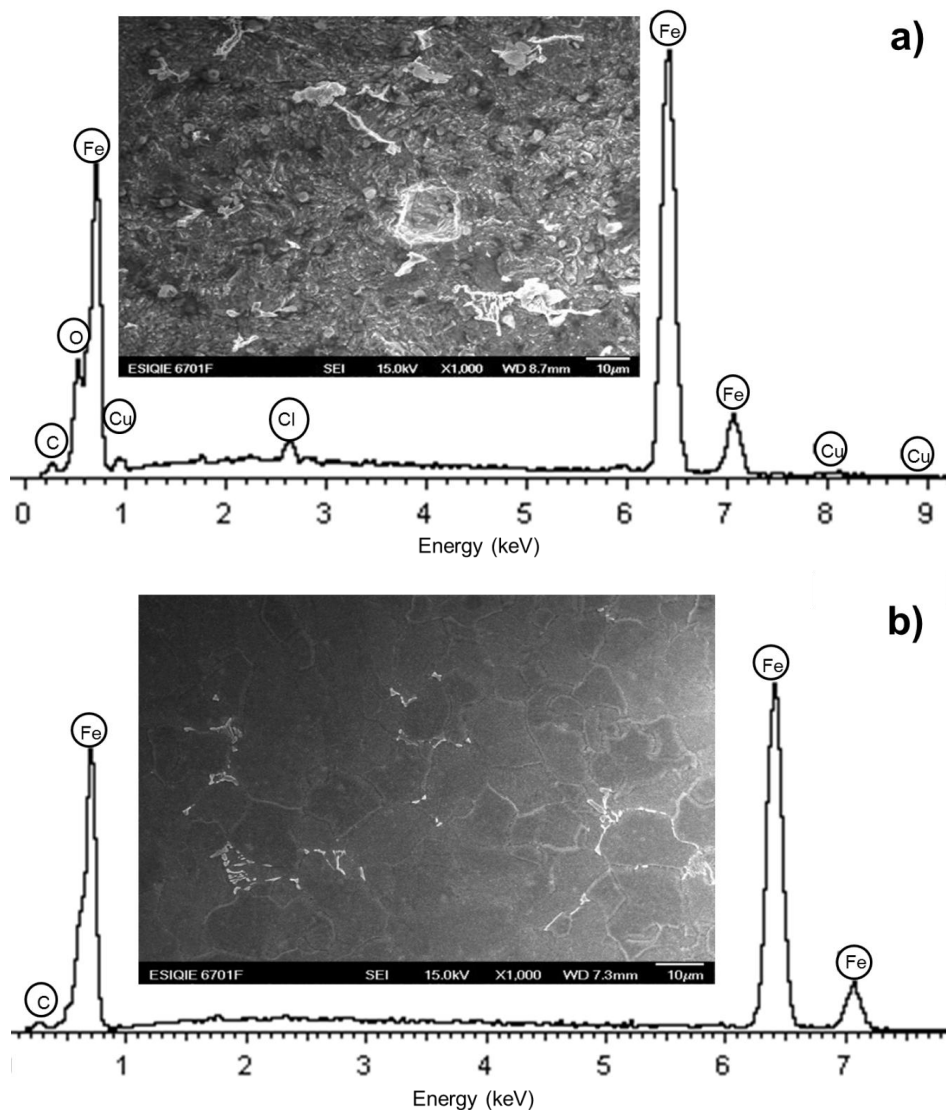


Figure 10. SEM micrographs and EDX spectrum for API 5L X52 steel: (a) after 12 h of immersion in 1 M HCl in absence of Cl and (b) with 100 ppm of DCA (c).

The elemental analysis indicates the presence of chlorine and a high concentration of oxygen, which are attributed to the formation of oxides/oxi-hydroxides and iron chlorides. In DCA presence, the surface damage is reduced considerably as shown in Figure 9 (c), having clearly two zones: one that presents corrosion products due to the presence of active sites and another one where a uniform morphology with clear microstructure evidence can be appreciated. The EDX spectrum indicates a remarkable reduction of the oxygen signal and the absence of chlorine, confirming that the steel surface features less corrosion products after adding DCA due to the formation of a CI protective film, responsible of its steel inhibiting action. Figures 10 (a) and (b) show the SEM images and EDX spectra of API 5L X52 steel after 4 h of immersion in 1 M HCl at 40 °C in absence (a) and presence of 100 ppm of DCA (b). Figure 10 (a) shows important surface roughness provoked by the steel dissolution. In addition to the presence of small dark areas distributed all over the surface that confirm localized corrosion of pitting type. The damage by surface corrosion in CI absence at 40 °C was higher than at

25 °C, although the micrograph in Figure 10 (a) was obtained at a shorter time. This fact confirms once again that the corrosion velocity is directly proportional to temperature. The EDX analysis shows the characteristic peaks of the elements that constitute the API 5L X52 steel sample; in addition, the presence of oxygen and chlorine in the spectrum suggests the formation of iron corrosion products. The SEM micrograph of steel immersed in 1 M HCl and 100 ppm of DCA, Figure 10(b), shows a homogeneous surface morphology, besides a possible type of localized corrosion, which allows to visualize clearly the surface grain limits, being this clear evidence of the DCA inhibition efficiency of the API 5L X52 steel exposed to hydrochloric acid. This statement is supported by the EDX spectrum where the oxygen and chlorine signals are absent, which are associated commonly with corrosion products.

4. CONCLUSIONS

The ionic liquid *N*-dimethyl-*N*-di(cocoalkyl) ammonium methyl sulfate (DCA) showed corrosion inhibition properties for the protection of API 5L X52 steel in aqueous 1 M HCl, which was confirmed by polarization curves. The DCA inhibition mechanism was attributed to the strong adsorption ability of this ionic liquid to form a protective layer on the metal surface, reducing the active sites and the steel dissolution at the anodic sites by the aggressive environment. The polarization curve results confirmed that DCA is a mixed-type corrosion inhibitor without clear preferences toward the anodic or cathodic side. The effects exerted by the temperature and time on the *IE* were strong, having the best result after 4 h and at 50 °C within the 96-99%; whereas the least *IE* was obtained at 0 h and 30 °C within the 50- 94% interval. The surface analysis in presence and absence of CI confirm that DCA inhibited the steel corrosion due to its adsorption on the steel surface. Its moderate thermal stability suggests that this compound may be considered for further studies to determine its upper level application as a corrosion inhibitor.

ACKNOWLEDGMENTS

The authors gratefully acknowledge Conacyt-Mexico for the sponsorship provided. Octavio Olivares-Xometl thanks SNI, BUAP-VIEP and Conacyt 167232 project. Paulina Arellanes-Lozada would like to thank ESQIE-IPN for the support provided.

References

1. A.A. Farag, M.R.N. El-Din, *Corros. Sci.*, 64 (2012) 174-183.
2. S.K. Shukla, L.C. Murulana, E.E. Ebenso, *Int. J. Electrochem. Sci.*, 6 (2011) 4286-4295.
3. M. Javidi, S.B. Horeh, *Corros. Sci.*, 80 (2014) 213-220.
4. H. Bentrah, Y. Rahali, A. Chala, *Corros. Sci.*, 82 (2014) 426-431.
5. M.A. Hegazy, M. Abdallah, M.K. Awad, M. Rezk, *Corros. Sci.*, 81 (2014) 54-64.
6. M. Finšgar, J. Jackson, *Corros. Sci.*, 86 (2014) 17-41.
7. I. Lozano, E. Mazario, O. Olivares-Xometl, N.V. Likhanova, P. Herrasti, *Mater. Chem. Phys.*, 147 (2014) 191-197

8. D. Coleman, N. Gathergood, *Chem. Soc. Rev.*, 2010, 39, 600–637.
9. M.C. Bubalo, K. Radošević, I.R. Redovniković, J. Halambek, V.G. Srček, *Ecotox. Environ. Safe.*, 99 (2014) 1-12.
10. E. Kowsari, M. Payami, R. Amini, B. Ramezanzadeh, M. Javanbakht, *Appl. Surf. Sci.*, 289 (2014) 478- 486.
11. P. Huang, J.A. Latham, D.R. MacFarlane, P.C. Howlett, M. Forsyth, *Electrochim. Acta.*, 110 (2013) 501– 510.
12. M. Aliofkhazraei, *Developments in Corrosion Protection, Chapter 19: Environmentally Friendly Corrosion Inhibitors*, InTech, 2014.
13. E. Kowsari, M. Payami, R. Amini, B. Ramezanzadeh, M. Javanbakht, *Appl. Surf. Sci.*, 289 (2014) 478-486,
14. N.V. Likhanova, M.A. Domínguez-Aguilar, O. Olivares-Xometl, N. Nava-Entzana, E. Arce, H. Dorantes, *Corros. Sci.*, 52 (2010) 2088-2097.
15. D. Guzman-Lucero, O. Olivares-Xometl, R. Martínez-Palou, N.V. Likhanova, M.A. Domínguez-Aguilar, V. Garibay-Febles, *Ind. Eng. Chem. Res.*, 50 (2011) 7129-7140,
16. T. Tüken, F. Demir, N. Kıcır, G. Sığircık, M. Erbil, *Corros. Sci.*, 59 (2012) 110-118.
17. J. Sun, P.C. Howlett, D.R. MacFarlane, J. Lin, M. Forsyth, *Electrochim. Acta.*, 54 (2008) 254-260.
18. X. Li, S. Deng, H. Fu, *Corros. Sci.*, 53 (2011) 1529-1536.
19. T. Gu, Z. Chen, X. Jiang, L. Zhou, Y. Liao, M. Duan, H. Wang, Q. Pu, *Corros. Sci.*, doi.org/10.1016/j.corsci.2014.10.004.
20. O. Olivares-Xometl, C. Lopez-Aguilar, P. Herrastí-Gonzalez, N.V. Likhanova, I. Lijanová, R. Martínez-Palou, J.A. Rivera-Marquez, *Ind. Eng. Chem. Res.*, 53 (2014) 9534-9543
21. C. Gabler, C. Tomastik, J. Brenner, L. Pisarova, N. Doerr, G. Allmaier, *Green Chem.*, 13 (2011) 2869-2877.
22. P.C. Howlett, J. Efthimiadis, P. Hale, G.A. van Riessen, D.R. MacFarlane, M. Forsyth, *J. Electrochem. Soc.*, 157 (2010) C392-C398.
23. I. Ahamad, R. Prasad, M.A. Quraishi, *Corros. Sci.*, 52 (2010) 933-942.
24. P. Morales-Gil, M.S. Walczak, R.A. Cottis, J.M. Romero, R. Lindsay, *Corros. Sci.*, 85 (2014) 109-114.
25. E.A. Flores, O. Olivares, N.V. Likhanova, M.A. Domínguez-Aguilar, N. Nava, D. Guzman-Lucero, M. Corrales, *Corros. Sci.*, 53 (2011) 3899-3913.
26. K.R. Ansari, M.A. Quraishi, A. Singh, *Corros. Sci.*, 79 (2014) 5-15,
27. O. Olivares, N.V. Likhanova, B. Gómez, J. Navarrete, M.E. Llanos-Serrano, E. Arce, J.M. Hallen, *Appl. Surf. Sci.*, 252 (2006) 2894-2909.
28. P. Mourya, S. Banerjee, M.M. Singh, *Corros. Sci.*, 85 (2014) 352-363.
29. A.A. Farag, M.R.N. El-Din, *Corros. Sci.*, 64 (2012) 174-183.

© 2015 The Authors. Published by ESG (www.electrochemsci.org). This article is an open access article distributed under the terms and conditions of the Creative Commons Attribution license (<http://creativecommons.org/licenses/by/4.0/>).